

# Static and Frequency Dependent Polarizabilities and Hyperpolarizabilities of $H_2S_n$

S. G. RAPTIS,<sup>1,2</sup> S. M. NASIOU,<sup>3</sup> I. N. DEMETROPOULOS,<sup>3</sup>  
M. G. PAPADOPOULOS<sup>1</sup>

<sup>1</sup>National Hellenic Research Foundation, 48 Vas. Constantinou Avenue, Athens 11635, Greece

<sup>2</sup>Chemical Engineering Department, National Technical University of Athens, Zografou Campus, Athens 15773, Greece

<sup>3</sup>Chemistry Department, University of Ioannina, Ioannina 45110, Greece

Received 17 February 1998; accepted 22 June 1998

**ABSTRACT:** The structure–polarization relationship was investigated in a series of polysulfanes,  $H_2S_n$ . The reported results demonstrate that the forms of change of the polarizability components,  $\alpha_{ii}$ , and the second hyperpolarizability components,  $\gamma_{iiii}$ , as well as the average values  $\alpha$  and  $\gamma$ , respectively, of  $H_2S_n$  with  $n$  are similar. This shows that polarizability components can be easily used to determine corresponding hyperpolarizability data. A remarkable change of the hyperpolarizabilities with the molecular geometry of  $H_2S_n$  was found. This result can be used for the design of nonlinear optical materials with optimum properties. The present study uses the flexible  $\sigma$  bonded  $H_2S_n$  and is complementary to the works that considered the effect of conformational changes of  $\pi$ -conjugated systems on their hyperpolarizabilities. The present computations were performed using the semiempirical approaches MNDO and MNDO/d, as well as *ab initio* methods with STO-3G, extended with polarization and diffuse functions, and  $[3s2p/7s5p2d]$  sets for  $H_2S_n$ . At the *ab initio* level, the electronic and the vibrational contributions to polarizabilities and hyperpolarizabilities were both computed for several members of  $H_2S_n$ . The frequency dependence of the above contributions and the static limit were discussed. Electron correlation was taken into account for several test cases using MP2 theory. The selected methods and the variety of the approximations on which they rely

Correspondence to: M. G. Papadopoulos; e-mail: mpapad@eie.gr

This article contains Supplementary Material available from the authors or via the Internet at <ftp.wiley.com/public/journals/jcc/suppmat/19/1698> or <http://journals.wiley.com/jcc/>

allow the systematic consideration of the effect of changes of the geometry of  $\text{H}_2\text{S}_n$  on their polarizabilities and second hyperpolarizabilities. © 1998 John Wiley & Sons, Inc. J Comput Chem 19: 1698–1715, 1998

**Keywords:** MNDO; MNDO/*d*; polarizabilities; hyperpolarizabilities;  $\text{H}_2\text{S}_n$

## Introduction

**P**olarizabilities and hyperpolarizabilities<sup>1</sup> have attracted the interest of an increasing number of researchers because they provide important information for molecular structure.<sup>2,3</sup> In addition, the hyperpolarizabilities are of great importance for the design of materials that have many applications (e.g., optical processing of information, optical computing etc.).<sup>4</sup> Design or selection of materials, which are likely to have the optimum properties, requires an in depth understanding of the structure–polarization relationship.

In this work we investigated the way the change of molecular geometry affects the polarizabilities and second hyperpolarizabilities of  $\text{H}_2\text{S}_n$ , which was selected as the model compound. The S—H and S—S bonds are of considerable importance in chemical and biological systems.<sup>5a,b</sup> Sulfur is also involved in derivatives with promising nonlinear electric properties.<sup>5c,d</sup> One notes that the structure–property relationships, which are used to guide one's efforts in molecular engineering,<sup>5e</sup> were investigated to a considerable extent in linear polyenes or in general in conjugated systems.<sup>5f–i</sup> In particular, the effect of conformational changes or disorders on the nonlinear optical properties was studied extensively in conjugated systems (see brief literature survey in later section). Thus, we systematically selected a set of conformational changes in the structure of  $\text{H}_2\text{S}_n$ , because the effect of disorders in this class of flexible systems has not been studied before, as far as we know. In addition, understanding of the implications of the geometry variations on the hyperpolarizabilities in the above nonplanar systems is complementary to that resulting from studies in planar conjugated systems. The selected polysulfanes could not be considered as nonlinear optical materials but rather as test models to analyze the effect of the above structural changes on the polarizabilities and hyperpolarizabilities of such materials.

For the present study we used semiempirical (MNDO<sup>6</sup> and MNDO/*d*<sup>7</sup>) and *ab initio* methods.

Correlation was taken into account at the MP2 level.<sup>8</sup> At the *ab initio* level the static and frequency dependent electronic and vibrational contributions of some members of the series  $\text{H}_2\text{S}_n$  were calculated. This allowed a comprehensive understanding of the nonlinear optical properties in this class of compounds. The significant contribution of the static vibrational second hyperpolarizability, compared with electronic contribution, is also documented.

## Computational Methods

Of primary importance for the present work are the trends and differences in the properties, because these are necessary for discussing the structure–polarization relationship. To check the adequacy of the employed semiempirical methods in order to approach the required goal, we performed extensive tests and comparisons using several theoretical techniques (semiempirical and *ab initio*) and the experimental results where they were available (Tables I, II).

At the semiempirical level we used the MNDO<sup>6</sup> and MNDO/*d*<sup>7</sup> methods. The latter involves *d* orbitals on S, due to which gives results of superior quality in comparison to those produced by the MNDO as will be shown. A detailed description of these methods is given in refs. 6a and 7.

At the *ab initio* level the properties of  $\text{H}_2\text{S}_n$  were computed using the GAMESS program<sup>9</sup> with the two following basis sets:

1. The STO-3G set, extended with polarization (p on H and d on S) and diffuse functions on both H(*s*) and S(*s*, *p*),<sup>9</sup> denoted by STO-3G\*\*++; and
2. The set (6s4p/14s10p4d)/[3s2p/7s5p2d] published by Sadlej.<sup>10a,b</sup>

The former was selected because it is a small set, which gives satisfactory  $\gamma$  values for  $\text{H}_2\text{S}_n$  in comparison to the Sadlej orbitals (Table II). The

TABLE I.  
Dipole Moment of H<sub>2</sub>S<sub>n</sub> (n = 1 – 9) Computed by Various Methods.

Compound	$\mu / \text{au}$					Experimental
	MNDO	MNDO / d	STO-3G**++	MP2 / STO-3G**++	[3s2p / 7s5p2d]	
H <sub>2</sub> S	0.582	0.407	0.677	0.671	0.445	0.383 ± 0.002 <sup>19a</sup> 0.353 <sup>a</sup> 0.369 <sup>a</sup> 0.386 <sup>a</sup> 0.433 ± 0.020 <sup>a</sup>
H <sub>2</sub> S <sub>2</sub>	0.639	0.465	0.716	0.703	0.479	
H <sub>2</sub> S <sub>3</sub>	0.236	0.227	0.223	0.217	0.183	
H <sub>2</sub> S <sub>4</sub>	0.307	0.130	0.390	0.369	0.237	
H <sub>2</sub> S <sub>5</sub>	0.607	0.386	0.675	0.638	0.468	
H <sub>2</sub> S <sub>6</sub>	0.408	0.326	0.398	0.376		
H <sub>2</sub> S <sub>7</sub>	0.119	0.004	0.192	0.180		
H <sub>2</sub> S <sub>8</sub>	0.548	0.320	0.623			
H <sub>2</sub> S <sub>9</sub>	0.525	0.380	0.538			

The properties of H<sub>2</sub>S<sub>n</sub> were computed using bond length and angles defined by model 3 (see text). The asterisks denote that polarization functions were used for H(p) and S(d). The two pluses mean that diffuse functions were employed for H(s) and S(sp) of H<sub>2</sub>S<sub>n</sub>.

<sup>a</sup> Gas phase values cited by McClellan.<sup>19b</sup>

functions reported by Sadlej are medium size polarized basis sets designed for the satisfactory calculation of dipole moments and polarizabilities.<sup>10a, b</sup>

The polarizability and hyperpolarizability values presented in this work were computed using the following methods:

1. A finite perturbation theory approach, which was used in connection with the MNDO technique<sup>6, 11</sup> and the ab initio procedure at the MP2 level<sup>8</sup>; and
2. Analytical methods implemented in the MNDO/d<sup>7</sup> and GAMESS,<sup>9</sup> which are used for the computation of the properties at the self-consistent field (SCF) level.

The vibrational polarizabilities and hyperpolarizabilities of H<sub>2</sub>S<sub>n</sub> (n = 1–3) were computed using the perturbation theoretic approach proposed by Bishop and Kirtman<sup>12a–c</sup> and implemented by Cohen et al.<sup>12d</sup> The required derivatives of the energy (second and third order), dipole moment (first and second order), polarizability (first and second order), and first hyperpolarizability (first order)<sup>12d</sup> were computed at the SCF level using CADPAC<sup>12e</sup> and the vibrational properties were calculated employing SPECTRO.<sup>12</sup>

The property values presented in this work are given in atomic units (au).<sup>12g</sup>

## Results and Discussion

The material presented in this section is organized in the following way: first a literature survey is presented; then the employed geometric models are discussed; followed by the analysis of the electronic dipole moment, polarizabilities, and second hyperpolarizabilities; and finally comments are made about the vibrational polarizabilities and hyperpolarizabilities.

### LITERATURE SURVEY

The structure–polarization relationship has been investigated in considerable detail in conjugated systems.<sup>13–15</sup> One may distinguish three themes on which the attention of the various workers is focused:

1. The derivation of scaling rules that connect the size (number of double bonds etc.) with the properties (polarizability or hyperpolarizability components or average values).<sup>13a, b, c, h, 14</sup>
2. The use of molecular geometry as a tool to achieve the required nonlinearities.<sup>13f, g</sup> Marder et al.<sup>13f</sup> showed that by reducing the bond length alternation (which is the average

TABLE II.  
Comparison of  $\beta$  for H<sub>2</sub>S<sub>n</sub> Determined by MNDO, MNDO/d, STO-3G\*\*+++, and MP2/STO-3G\*\*++.

Compound	$\beta(0; 0, 0) / \text{au}$			$\beta(-2\omega; \omega, \omega) / \text{au}$		
	MNDO <sup>a</sup>	MNDO/d <sup>a</sup>	STO-3G**++ <sup>a</sup>	MP2/STO-3G**++ <sup>b</sup>	[3s2p/7s5p2d] <sup>a</sup>	STO-3G**++ <sup>a,c</sup>
H <sub>2</sub> S	-72.389	-29.843	-12.488	-15.153	3.317	-19.295
H <sub>2</sub> S <sub>2</sub>	-102.871	-61.822	-4.815	-10.451	2.209	-14.864
H <sub>2</sub> S <sub>3</sub>	-51.356	-14.501	-2.275	-7.371	-13.013	-15.472
H <sub>2</sub> S <sub>4</sub>	-77.870	-100.263	-5.018	-8.195	18.834	4.699
H <sub>2</sub> S <sub>5</sub>	-152.300	-140.006	1.484	-5.376	10.439	2.635
H <sub>2</sub> S <sub>6</sub>	-94.456	-52.670	8.327	5.410		
H <sub>2</sub> S <sub>7</sub>	-53.587	92.425	1.012	2.646		16.005
H <sub>2</sub> S <sub>8</sub>	-166.911	-173.392	13.339	12.924		24.072
H <sub>2</sub> S <sub>9</sub>	-141.466	-106.219	15.143	14.418		12.948

The property values of this table were determined using for H<sub>2</sub>S<sub>n</sub>, bond lengths and angles optimized by MNDO (model 3).

<sup>a</sup> These results were determined by a perturbation theory method as implemented in MNDO/d<sup>7</sup> and GAMESS.<sup>9</sup>

<sup>b</sup> These data were calculated by a finite perturbation theory approach.

<sup>c</sup> The results of this column were computed at 694.3 nm unless otherwise specified.

<sup>d</sup> Value determined using dc-induced second harmonic generation in the gas phase.<sup>19a</sup>

difference in length between the single and double bonds<sup>13g</sup>), one gets large hyperpolarizabilities. It is thus demonstrated that geometry can be employed as a key factor to produce large nonlinearities.

3. The study of the effect of conformational changes or disorders on various properties of the electronic structure and in particular on the polarizabilities and hyperpolarizabilities.<sup>13d, e, i, 15a</sup>

It should be noted that the effect of conformational changes on the nonlinear optical properties has been studied using mainly conjugated systems. The present study, which employs four different models or conformations, allows us to trace and analyze the effect of regular and irregular changes in the geometry of H<sub>2</sub>S<sub>n</sub> on their  $\mu$ ,  $\alpha$  and  $\gamma$  as well as their development with  $n$ .

Two important review articles, which are related to some aspects of the present work, recently appeared. These were written by Bishop<sup>15b</sup> and Kirtman and Champagne.<sup>15c</sup>

## GEOMETRIC MODELS

We used several models for H<sub>2</sub>S<sub>n</sub> in order to study the effect of changes in the molecular geometry on the properties of interest ( $\mu$ ,  $\alpha$  and  $\gamma$ ). The first of those, *model 1*, assumes that the molecules are planar (Fig. 1) and initially all dihedral angles are set at 180°. The optimization is performed having as variables the bond lengths (H — S and S — S) and angles (S — S — S and H — S — S), constraining the dihedrals to the set value. The bond lengths S — S and angles S — S — S of a given H<sub>2</sub>S<sub>n</sub> were not constrained to have the same value. In *model 2* the initial geometry for each molecule H<sub>2</sub>S<sub>n</sub> is set as in model 1. The geometry optimization is performed for all bonds, angles, and dihedral angles (unconstrained minimization), yielding conformers that can be described as helices and segments of helices with reverse turns. Helices are secondary structures built from a sequence of consecutive dihedral angles with approximately equal values, say  $g$  (in our case approximately 90°), then  $gggggg$  is the string describing a nine atom helix. Reverse turns are the intervention to this consequence at some point by a  $-g$  dihedral angle producing a string  $ggg-ggg$ .

*Model 3* assumes a helical structure (Fig. 1). This configuration was adopted because it was thought

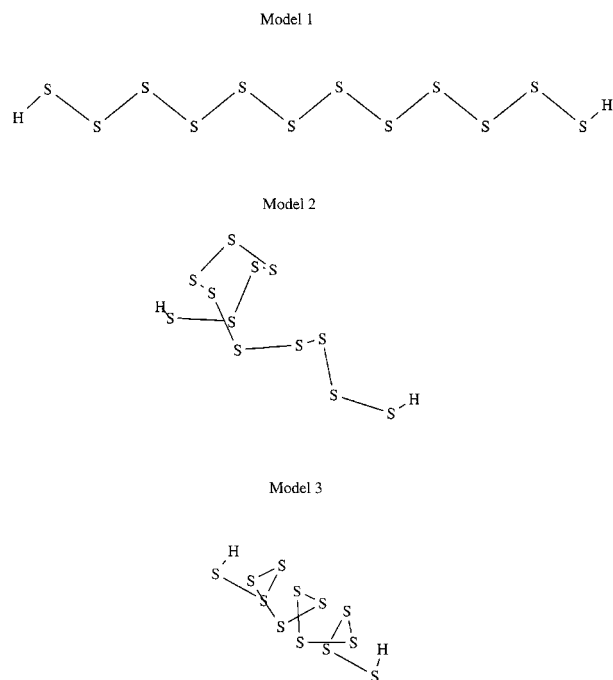


**FIGURE 1.** The structure of  $H_2S_n$ , models 1–3, using  $H_2S_{12}$  as an example.

that it is likely to be the most favorable, using the energy as a criterion.<sup>16a</sup> This hypothesis was confirmed after detailed computations that were performed in the following steps using  $H_2S_{12}$  as a test case (Fig. 2). First, the suite of programs GMMX<sup>16b,e</sup> was used for the optimization. This employs the MM2 (Molecular Mechanics, program 2), force field.<sup>16c,d</sup> It searches the conformational space using the stochastic procedure described by Saunders et al.<sup>16e</sup> From these computations resulted the six, lower lying in energy, conformers. Subsequently, the GMMX generated conformers were geometry optimized with the MNDO<sup>6</sup> Hamiltonian. These calculations showed that the helical structure is associated with the global energy minimum and the conformers depicted as helices segmented by reverse turns are local energy minima. In addition, an MNDO systematic conformational search was performed for the  $H_2S_{12}$  molecule; the outcome verified the helical structure as the most stable conformation for  $H_2S_{12}$ . All model 3 stationary points ended up with a force matrix calculation; no imaginary frequencies were found, hence,  $H_2S_n$  helical structures are true minima. Greenwood and Earnshaw<sup>17</sup> noted that "...it is now established that fibrous S consists of infinite chains of S atoms arranged in parallel helices." Similar

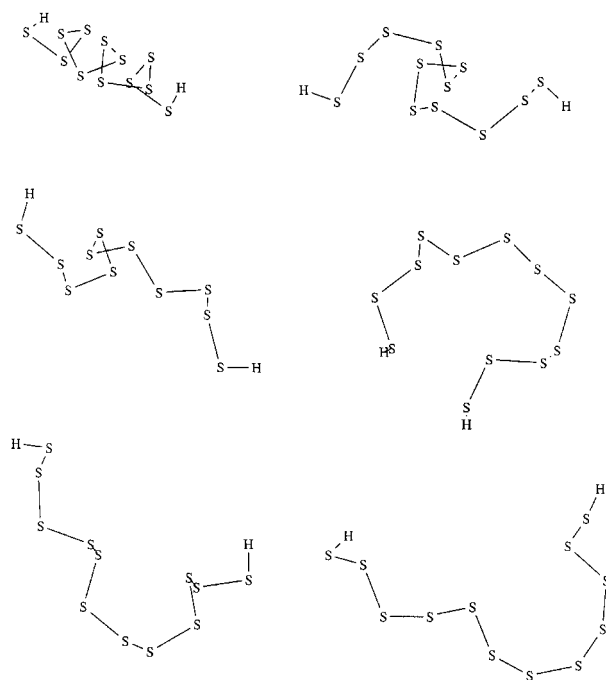


**FIGURE 2.** The six conformers of lower energy for  $H_2S_{12}$ .

information is also provided by Cotton and Wilkinson.<sup>18a</sup>

Summarizing the main features of models 2 and 3, we note that calculations for the structure of  $H_2S_n$ , which were performed using model 2, produced helices and helices with reverse turns while only helical geometries were computed using model 3.

*Model 4* (Fig. 3) involves structures in the form of closed chains. We consider  $S_8$ ,  $S_{12}$ ,  $S_{16}$ , and  $S_{20}$ . The geometries of models 1–4 were optimized using the MNDO<sup>6</sup> approach.

The semiempirical computations using models 1–4 at the MNDO level were performed using MOPAC 6.0.<sup>6b</sup> The keyword POLAR, which was employed for the calculations of the polarizabilities and hyperpolarizabilities, leads to the orientation of the molecule so that the tensor of inertia is diagonal. The coordinates of the first nine molecules, which were used for the *ab initio* calculations, are given as supplementary material. However, all the above structural data (models 1–4) can also be provided on request.

A natural bond order analysis on  $H_2S_2$  and  $H_2S_3$  confirmed the  $\sigma$  nature of the S—S bond. The  $3d$  atomic orbitals of the sulfur atoms, which play a significant role on hypervalent sulfur com-

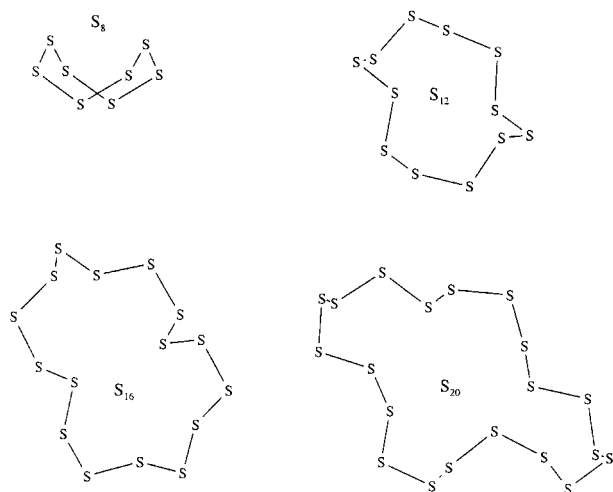


**FIGURE 3.** The structure of  $\text{S}_n$ , where  $n = 8, 12, 16$ , and  $20$ .

pounds,<sup>18b</sup> are of a minor importance (1.3%) in the considered  $\text{H}_2\text{S}_n$ . The stability of the helical conformation can be explained by the advantageous orientation of the sulfur lone pairs that, in this position, have minimum repulsion energy.<sup>18c,d</sup> The lack of  $\pi$  bonds is the main reason for the smaller second hyperpolarizabilities of polysulfanes in comparison with those of polyenes.<sup>5g</sup> The  $\pi$  bond that serves as a bridge for the flow of electrons does not exist in  $\text{H}_2\text{S}_n$  and thus the  $\pi$  electron delocalization along the chain direction<sup>18e</sup> that accounts for the large second hyperpolarizabilities of the conjugated systems is absent.

In the following paragraphs a comparative study of the dipole moment, polarizability, and hyperpolarizabilities of  $\text{H}_2\text{S}_n$  computed with MNDO, MNDO/*d*, and *ab initio* methods is presented (Tables I–III). For the geometries of  $\text{H}_2\text{S}_n$ , the above-defined models 1–3 will be used. Thus, the effect of the molecular geometries on the properties of interest will be analyzed.

## DIPOLE MOMENTS

It is likely that the best dipole moment values are those given by the Sadlej basis set.<sup>10</sup> This hypothesis is supported by comparing the computed dipole moment value of  $\text{H}_2\text{S}$ , using the methods employed in the present work, with the experimentally determined one<sup>19a,b</sup> (Table I). However, the variation of  $\mu$  of  $\text{H}_2\text{S}_n$  as a function of  $n$  is correctly described by the MNDO method (Table I, Fig. 4).

## POLARIZABILITIES

### Frequency Dependent Values, $\alpha(-\omega; \omega)$

The frequency dependent polarizabilities of  $\text{H}_2\text{S}_n$  were computed using the STO-3G\*\*++ (for  $n \leq 9$ ) and  $[3s2p/7s5p2d]$  (for  $n \leq 5$ ) basis sets. The results are shown in Table II. The dynamic polarizability of  $\text{H}_2\text{S}$  was calculated at four frequencies. One observes that there is a reasonable agreement between the computed and the experimental results (Table II). Figure 5 presents the variation of  $\alpha(-\omega; \omega)$  for  $\text{H}_2\text{S}_4$  as a function of the frequency. From the results of Table II we observe that the ratio  $\alpha(-\omega; \omega)/\alpha(0; 0)$ , at  $\lambda = 694.3$  nm, for increasing  $n$  ( $\text{H}_2\text{S}_n$ ), is approximately constant for both the employed basis sets (STO-3G\*\*++ and  $[3s2p/7s5p2d]$ ). This constant is approximately 1.03 for STO-3G\*\*++.

### Static Values, $\alpha(0; 0)$

We observe that (Table II)

$$\begin{aligned} \alpha[3s2p/7s5p2d] &> \alpha[\text{MP2/STO-3G}^{**++}] \\ &> \alpha[\text{STO-3G}^{**++}] \\ &> \alpha[\text{MNDO}/d] > \alpha[\text{MNDO}]. \end{aligned}$$

The difference

$$\Delta\alpha = \alpha(\text{MNDO}/d) - \alpha(\text{MNDO})$$

is small. For  $n = 1, 4$ , and  $9$ ,  $\Delta\alpha = 1.22, 2.4$  and  $0.0$  au, respectively. Thus, for  $n \geq 9$ , MNDO and MNDO/*d* most likely give the same polarizability values for  $\text{H}_2\text{S}_n$ . From the STO-3G\*\*++ results we observe that the correlation contribution increases with  $n$ . For  $\text{H}_2\text{S}_7$  this is 9.4%. The ratio

$$\alpha[3s2p/7s5p2d]/\alpha[\text{MNDO or MNDO}/d]$$

for  $\text{H}_2\text{S}_n$  decreases with  $n$ .

The polarizability values of  $\text{H}_2\text{S}_n$  computed with the MNDO are now discussed. In general we observe that  $P(n+1) > P(n)$ , where  $P = \alpha_{xx}, \alpha_{yy}, \alpha_{zz}$  and  $\alpha^{1a}$  (Fig. 6). However, there are several exceptions to the above trend, most of which are observed for model 2. We found that for model 1 we have (Fig. 6)

$$\alpha_{xx} \gg \alpha_{yy} > \alpha_{zz}.$$

For models 2 and 3

$$\alpha_{xx} \gg \alpha_{yy}$$

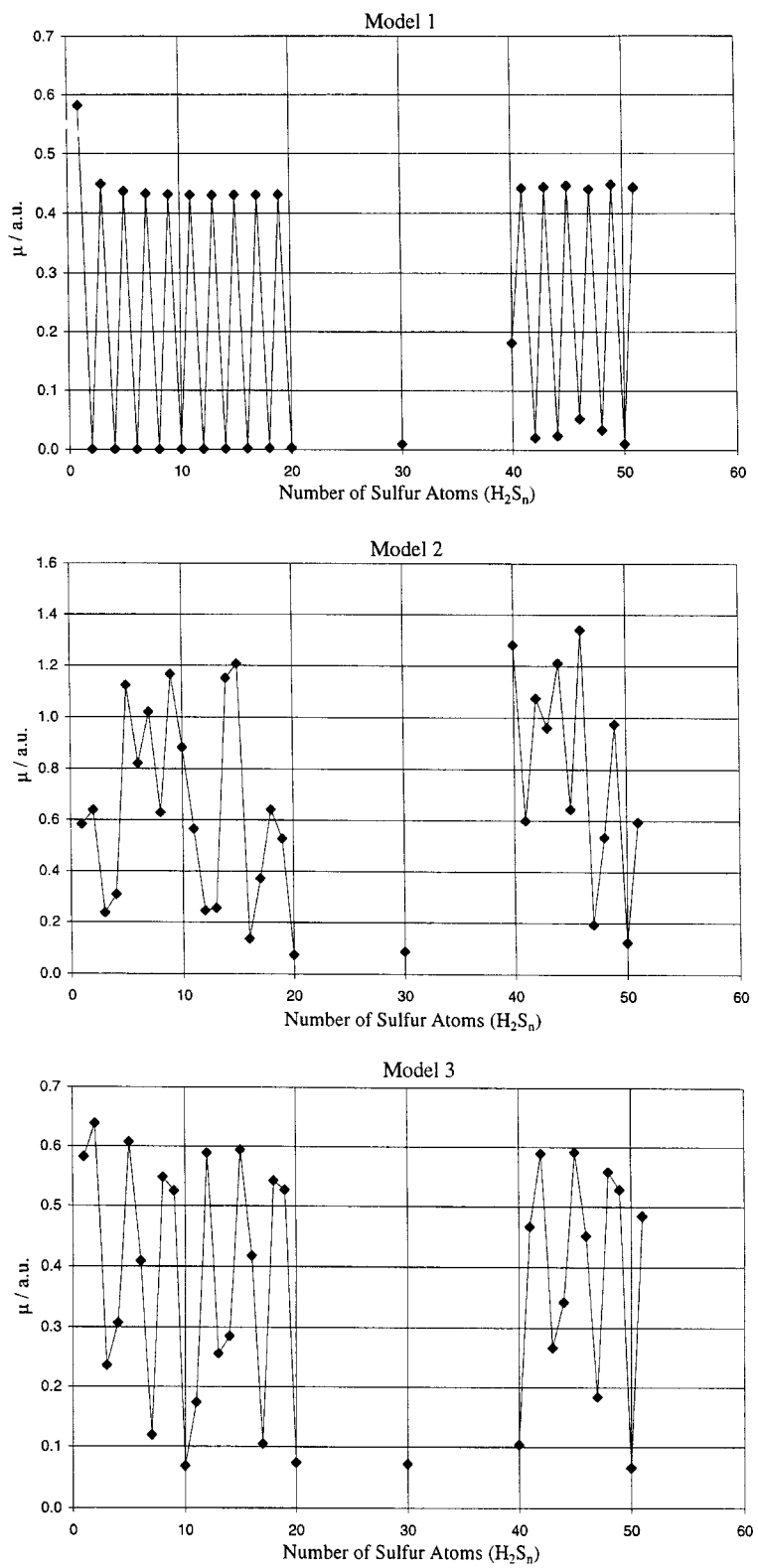


**FIGURE 4.** The dipole moment of  $H_2S_n$  (determined using the MNDO method) as a function of  $n$  for models 1–3.

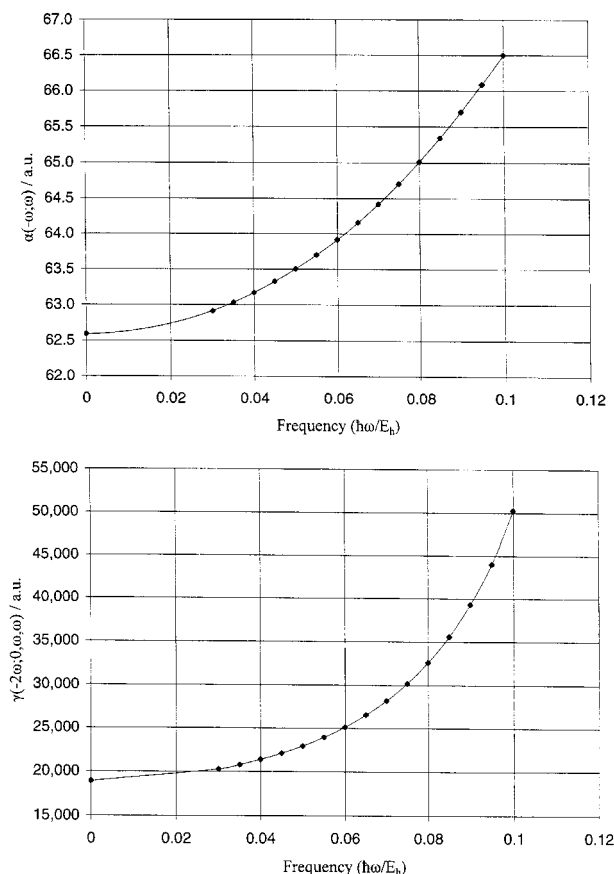


**FIGURE 5.** Plot of  $\alpha(-\omega; \omega)$  and  $\gamma(-2\omega; 0, \omega, \omega)$  of  $\text{H}_2\text{S}_4$  (STO-3G\*\*++) versus the frequency.

and in most cases the values of  $\alpha_{yy}$  and  $\alpha_{zz}$  differ very little. For models 1 and 3  $\alpha_{xx}$ ,  $\alpha_{yy}$ ,  $\alpha_{zz}$ , and  $\alpha$  change linearly with  $n$  for  $n \geq 40$ . However, it would be a reasonable approximation to consider that this holds for even smaller values of  $n$  (e.g., for  $n \geq 15$ ). The change of the polarizability properties (e.g.,  $\alpha_{xx}$ ,  $\alpha$ ) with  $n$  for model 2 presents several irregularities (Fig. 6), which are induced by the irregularities in the structure. The dependence of the longitudinal polarizability and second hyperpolarizability on the chain length in conjugated hydrocarbons has been discussed by various authors (e.g., ref. 5g). In a more recent study Tretiak et al.<sup>14</sup> connected the  $j$ th order off-resonant polarizabilities of conjugated polymers with the number of carbon atoms, the bond length alternation, and the exciton coherence size.

Employing the three  $\alpha$  values (models 1–3) of  $\text{H}_2\text{S}_n$ , we calculated the averaged values using a

Boltzmann distribution<sup>19c</sup>

$$P_{\text{av}} = \sum_i P_i \exp(-H_f^0(i)/kT) / \sum_i \exp(-H_f^0(i)/kT), \quad (1)$$

where  $P$  denotes the  $\alpha$  or  $\gamma$  values;  $i$  defines the model (1–3);  $H_f^0$ ,  $k$ , and  $T$  are the heat of formation, the Boltzmann constant, and temperature (300 K), respectively. The plot of average values,  $\alpha_{\text{av}}$ , of  $\text{H}_2\text{S}_n$  versus  $n$  is shown in Figure 7. It has been found that  $\alpha_{\text{av}}$  of  $\text{H}_2\text{S}_n$  are close to the polarizability values computed using model 3. This is due to the fact that model 3 gives structures of lower energy in comparison to those produced by models 1 and 2. (However, some exceptions have been observed, e.g., for  $\text{H}_2\text{S}_n$ , where  $n = 13, 19$ , and 20, models 2 and 3 have approximately, the same energy.)

We found that the molecular shape greatly affects the magnitude of the polarizability and, in particular, the second hyperpolarizability. This is confirmed by comparing the  $\alpha$  values of model 4 with those of models 1–3. It is found that model 4, which involves closed chains, has a smaller  $\alpha$  than models 1–3 (Table III).

### FIRST HYPERPOLARIZABILITIES

We now discuss in some detail the first hyperpolarizability of  $\text{H}_2\text{S}$  for which there are reliable experimental and *ab initio* results. Sekino and Bartlett<sup>19d</sup> used the polarizability consistent basis set proposed by Sadlej<sup>10a,b</sup> and two extended versions of it at various levels of theory [SCF/TDHF, CCSD(T), etc.] and found for  $\text{H}_2\text{S}$  that at the SCF/TDHF  $\beta > 0$ , while at the CCSD(T) level their computed value is negative and agrees satisfactorily with the dc-SHG measurement of Ward and Miller.<sup>19a</sup> Thus, the great importance of the correlation contribution for  $\beta$  of  $\text{H}_2\text{S}$  is clear. This observation explains why our SCF results, static and dynamic, computed with Sadlej's basis set are not in satisfactory agreement with the experimental value (Table II). It may be fortuitous, but still pleasant, to observe that the STO-3G\*\*++ (static)  $\beta$  is in good agreement with the experimental value. The MP2/STO-3G\*\*++ and the frequency dependent STO-3G\*\*++  $\beta$  values are less satisfactory. Using the STO-3G\*\*++ results as reference, we observe that the MNDO and MNDO/ $d$  give  $\beta$  values that do not even have the right sign. Shelton and Rice<sup>3i</sup> noted that some widely used semiempirical methods (AM1, PM3, MNDO, etc.)



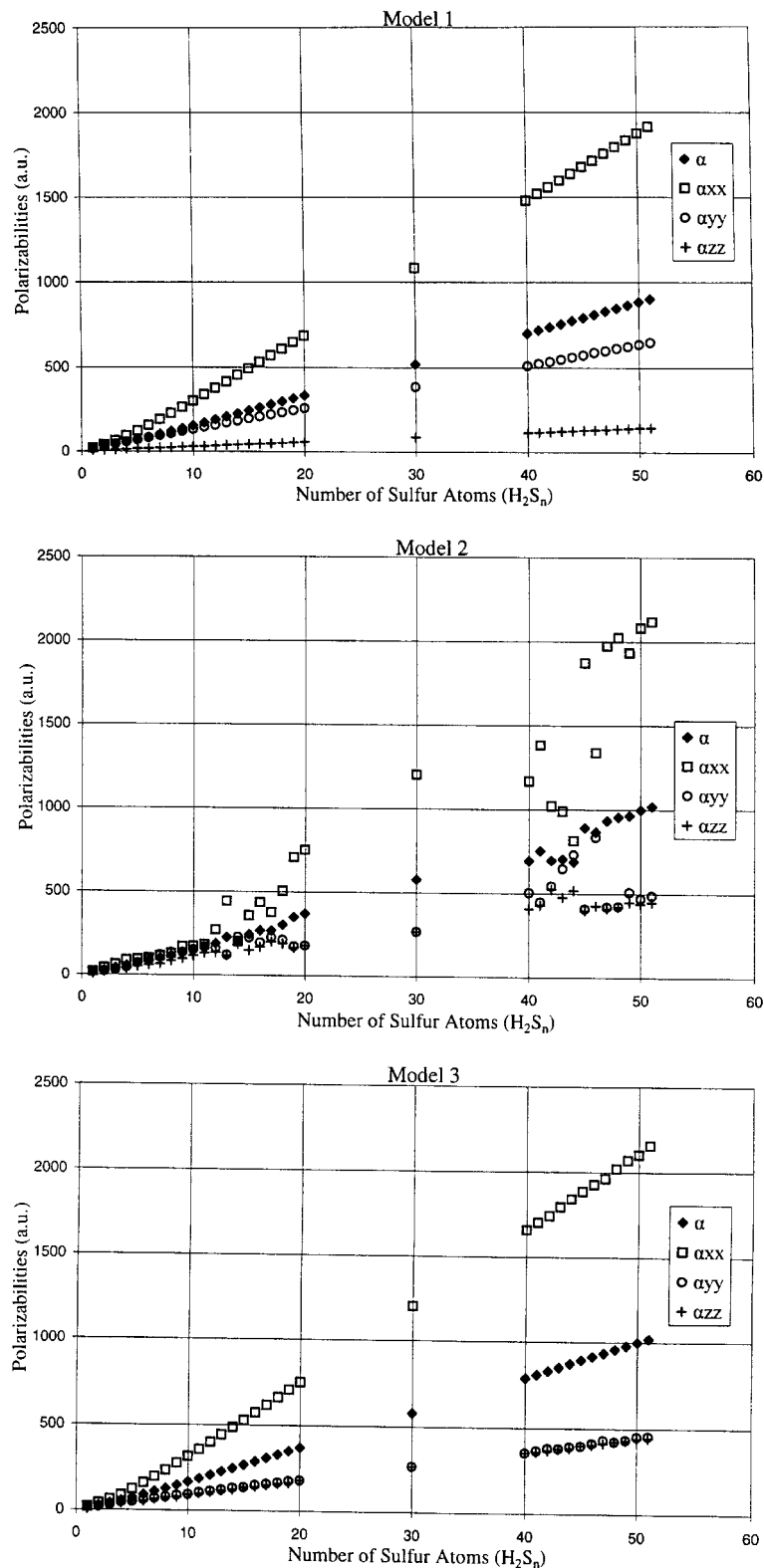


**FIGURE 6.** The polarizabilities ( $\alpha_{xx}$ ,  $\alpha_{yy}$ ,  $\alpha_{zz}$  and  $\alpha$ ) of models 1, 2, and 3. The results were calculated using the MNDO method.

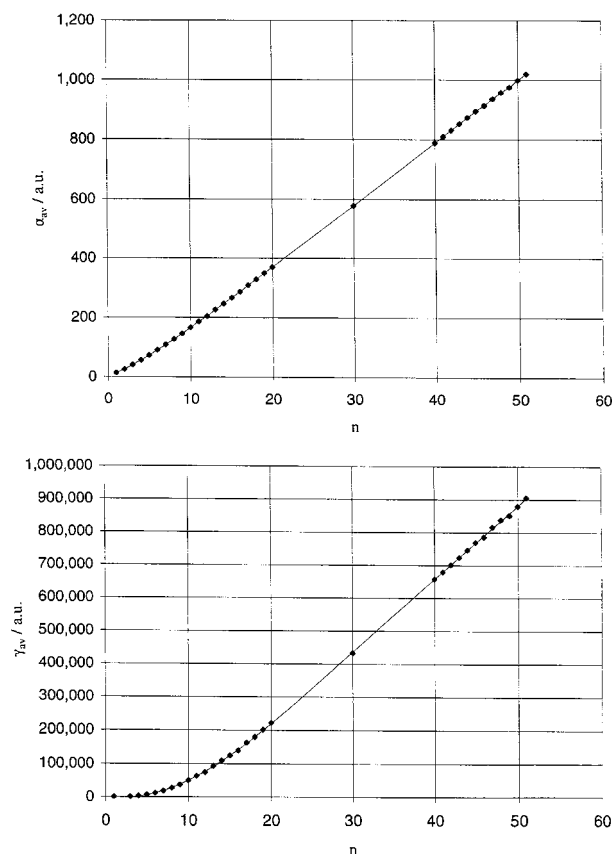


**FIGURE 7.** Plot of  $\alpha_{av}$  and  $\gamma_{av}$  [eq. (1)] versus  $n$  ( $\text{H}_2\text{S}_n$ ). The results were computed employing the MNDO method.

"...are not reliable for either the quantitative or the qualitative determination..." of the first hyperpolarizabilities. At least part of this deficiency is due to the overestimation of  $\beta_{zzz}$  at the expense of  $\beta_{zzx}$  and  $\beta_{zyy}$ .<sup>3i</sup> Taking into account the above observations, we shall not proceed to report and analyze the  $\beta$  values of  $\text{H}_2\text{S}_n$  for  $n > 11$ , using the MNDO or MNDO/*d* methods, because it has been shown that their reliability for the first hyperpolarizability is questionable. For completeness it is added that Malagoli and Thiel<sup>7c</sup> developed an extended version of MNDO and MNDO/*d* where  $2p$  functions for *H* are also used. They concluded that "The resulting specialized MNDO and MNDO/*d* treatments...are not useful for  $\beta$ ." (These methods, however, give reasonable polarizability values and reproduce trends in the second hyperpolarizabilities.)

## SECOND HYPERPOLARIZABILITIES

### dc-Electric Field Induced Second Harmonic Generation: $\gamma(-2\omega; 0, \omega, \omega)$

It is observed that the computed  $\gamma(-2\omega; 0, \omega, \omega)$  for  $\text{H}_2\text{S}$  is in fair agreement with the available experimental value measured by Ward and Miller<sup>19a</sup> (Table II). In Figure 5 we present the variation of  $\gamma(-2\omega; 0, \omega, \omega)$  of  $\text{H}_2\text{S}_4$  as a function of the frequency (the STO-3G\*\*++ basis set was employed). It is observed that for a given change in frequency, the resulting effect in  $\gamma(-2\omega; 0, \omega, \omega)$  is larger than that in  $\alpha(-\omega; \omega)$ . The ratio  $\gamma(-2\omega; 0, \omega, \omega)/\gamma(-0; 0, 0, 0)$  initially decreases and then stabilizes at 1.4 for  $n \geq 6$  (STO-3G\*\*++ ; Table II).

### Static Values: $\gamma(0; 0, 0, 0)$ .

From the results of Table III one observes that  $\gamma(\text{H}_2\text{S}_{n+1}) - \gamma(\text{H}_2\text{S}_n)$ , at both the STO-3G\*\*++ and the MP2/STO-3G\*\*++ , pass through a minimum. It would be perhaps appropriate to add that this basis may not be particularly good for treating correlation effects.

We observe that MNDO gives second hyperpolarizabilities for  $\text{H}_2\text{S}$  and  $\text{H}_2\text{S}_2$  having the wrong sign (they should be positive; Table II). As  $n$  increases the discrepancy of the semiempirical (MNDO and MNDO/*d*) results ( $\gamma$ ) with those determined by *ab initio* methods decreases. For certain value of  $n$  there is a crossing (Table II), for example, for  $n = 5$

$$\gamma(\text{MNDO}/d) < \gamma(\text{Sadlej}),$$

but for  $n = 7$

$$\gamma(\text{MNDO}/d) > \gamma(\text{Sadlej}).$$

The crossing between the MNDO  $\gamma$  values and those computed with the Sadlej basis set occurs for  $10 < n < 11$ . However, the major point of interest in this work is to semiquantitatively show the effect of geometry variations on the polarizabilities and hyperpolarizabilities of  $\text{H}_2\text{S}_n$  and this task can be accomplished satisfactorily by the MNDO method (Table III).

The second hyperpolarizabilities of  $\text{H}_2\text{S}_n$  calculated with the MNDO method will now be discussed. They take values that greatly depend on the adopted geometry. Thus, for  $\text{H}_2\text{S}_n$ , where  $n =$

TABLE III.  
Comparison of  $\alpha$  and  $\gamma$  for  $\text{H}_2\text{S}_n$  ( $n = 1 - 7$ ) Determined by MNDO, MNDO/ $d$ , STO-3G\*\*+++, and MP2/STO-3G\*\*++.

Compound	$\alpha(0; 0) / \text{au}$				$\alpha(-\omega; \omega) / \text{au}$				Exp. <sup>d</sup>
	MNDO <sup>a</sup>	MNDO/ $d^a$	STO-3G**++ + <sup>a</sup>	MP2/STO-3G**++ + <sup>b</sup>	[3s2p/7s5p2d] <sup>a</sup>	STO-3G**++ + <sup>a,c</sup>	[3s2p/7s5p2d] <sup>a,c</sup>		
H <sub>2</sub> S	9.98	11.2	14.1	14.6	23.2	14.5	24.3 <sup>e</sup> 24.2 <sup>f</sup> 23.8 <sup>g</sup> 23.7 <sup>h</sup> 41.4 61.2 81.6 103	26.0 <sup>e</sup> 25.9 <sup>f</sup> 25.5 <sup>g</sup>	
H <sub>2</sub> S <sub>2</sub>	22.4	24.4	28.2	29.7	40.5	29.0			
H <sub>2</sub> S <sub>3</sub>	37.2	39.5	45.8	49.5	59.8	47.0			
H <sub>2</sub> S <sub>4</sub>	53.0	55.4	62.6	68.2	79.6	64.2			
H <sub>2</sub> S <sub>5</sub>	69.8	71.9	79.7	87.4	100	81.8			
H <sub>2</sub> S <sub>6</sub>	87.4	89.2	97.3	107		99.8			
H <sub>2</sub> S <sub>7</sub>	106	107	115	127	144	118			
H <sub>2</sub> S <sub>8</sub>	124	125	133	147		137			
H <sub>2</sub> S <sub>9</sub>	144	144	151	168	190	156			
$\gamma(0; 0, 0, 0) \times 10^{-2} / \text{au}$									
H <sub>2</sub> S	-1.98	0.04	35.0	43.8	53.8	53.1	133 <sup>e</sup> 117 <sup>f</sup> 85.5 <sup>g</sup> 78.2 <sup>h</sup> 119	103.4 ± 0.69 <sup>h,i</sup>	
H <sub>2</sub> S <sub>2</sub>	-5.02	15.9	72.1	95.7	83.2	105			
H <sub>2</sub> S <sub>3</sub>	9.07	58.7	139	202	136	199			
H <sub>2</sub> S <sub>4</sub>	31.7	108	190	284	181	267			
H <sub>2</sub> S <sub>5</sub>	65.7	172	244	377	230	343			
H <sub>2</sub> S <sub>6</sub>	117	256	301	477		421			
H <sub>2</sub> S <sub>7</sub>	188	358	358	578	342	501			
H <sub>2</sub> S <sub>8</sub>	275	474	419	688		587			
H <sub>2</sub> S <sub>9</sub>	378	605	483	848	479	677			

The property values of this table were determined using for  $\text{H}_2\text{S}_n$ , bond lengths and angles optimized by MNDO (model 3).

<sup>a</sup> These results were determined by a perturbation theory method as implemented in MNDO/ $d$ <sup>7</sup> and GAMESS.<sup>9</sup>

<sup>b</sup> These data were calculated by a finite perturbation theory approach.

<sup>c</sup> The results of this column were computed at 694.3 nm unless otherwise specified.

<sup>d</sup> The cited mean molecular polarizability values<sup>26</sup> were derived by a critical evaluation of literature data.

<sup>e</sup> At 488 nm.<sup>26</sup>

<sup>f</sup> At 514.5 nm.<sup>26</sup>

<sup>g</sup> At 632.8 nm.<sup>26</sup>

<sup>h</sup> At 694.3 nm.

<sup>i</sup> Method: dc-electric field induced second harmonic generation in the gas phase.<sup>19a</sup>

1–51, the computed values are in atomic units (Fig. 8):

$$-0.198 \times 10^3 \leq \gamma \leq 0.73 \times 10^5 \quad \text{model 1,}$$

$$-0.198 \times 10^3 \leq \gamma \leq 9.05 \times 10^5 \quad \text{model 2,}$$

$$-0.198 \times 10^3 \leq \gamma \leq 9.05 \times 10^5 \quad \text{model 3.}$$

Figure 8 clearly shows that the dominant component in all three models is  $\gamma_{xxxx}$ . In several cases the absolute values of  $\gamma_{xyyy}$  and  $\gamma_{xxzz}$  are larger than those of  $\gamma_{yyyy}$  and  $\gamma_{zzzz}$ . In particular, this was found for  $n \geq 14$  of model 1. The variation of the components  $\gamma_{xyyy}$ ,  $\gamma_{xxzz}$ , and  $\gamma_{yyzz}$  as a function of  $n$  ( $\text{H}_2\text{S}_n$ ) is given as supplementary information (Fig. A).

The geometry adopted in model 1 shows that by varying  $\gamma$  versus  $n$  we observe one local minimum for  $n = 7$  (Fig. 9). Model 2 shows that variation of  $\gamma$  versus  $n$  presents several irregularities, while model 3 shows a smooth increase of  $\gamma$  with  $n$  (Fig. 9). In models 2 and 3,  $\gamma$  varies within the same bounds, although the change of  $\gamma$  as a function of  $n$  presents many dissimilarities in the two models. Models 1 and 3 differ widely in the absolute values of  $\gamma$ ; for example, for  $\text{H}_2\text{S}_{51}$

$$\gamma(\text{model 3})/\gamma(\text{model 1}) = 12.4.$$

The second hyperpolarizabilities of molecules with structures described by model 4 are smaller than those of molecules with geometries given by models 2 and 3, but larger than the hyperpolarizabilities of molecules that belong to model 1 (Table IV). In Figure 7 the  $\gamma_{av}$  of  $\text{H}_2\text{S}_n$  versus  $n$  is presented. The averaged values were calculated using eq. (1). We found that  $\gamma_{av}$  of  $\text{H}_2\text{S}_n$  is close to the  $\gamma$  of molecules, having structures that belong to model 3. The explanation of this observation was discussed in connection with the plot of  $\alpha_{av}$  versus  $n$ .

From the results in Figures 6 and 8 one deduces that there is a similarity in the change of  $\alpha_{ii}$  and  $\gamma_{iiii}$  of  $\text{H}_2\text{S}_n$  with  $n$ , which may be explained by taking into account that there is no charge transfer in the considered compounds. A similar trend is found for the pair  $\alpha/\gamma$ . This observation may be used to predict  $\gamma$  (or  $\gamma_{iiii}$ ) from  $\alpha$  (or  $\alpha_{ii}$ ). For example, using the  $\alpha$  values of  $\text{H}_2\text{S}_n$ ,  $n = 13$ –20 and 30, we predicted the  $\gamma$  values of  $\text{H}_2\text{S}_n$ ,  $n = 1$ –12 and 40–51 for models 1–3. The computed (MNDO) and the predicted values are shown in Figure 10.

We found that the  $\alpha$  and  $\gamma$  of  $\text{H}_2\text{S}_n$  vary with  $n$  following a completely different pattern than that of  $\mu$  (Figs. 4, 6, 8).

## VIBRATIONAL POLARIZABILITIES AND HYPERPOLARIZABILITIES

The properties discussed in the previous sections were the electronic contributions. The following analysis refers to the vibrational contributions to the polarizabilities and second hyperpolarizabilities. The superscripts e and v will be used to denote the electronic and vibrational contributions respectively (e.g.,  $\gamma^e$  and  $\gamma^v$ ).

There is a growing body of evidence that suggests that static  $\gamma^v$  is not negligible. Some well-known cases taken from the excellent review article of Bishop<sup>20</sup> are  $\text{SF}_6^{12a}$ , where the vibrational contribution is 20 times larger than the electronic and  $\text{H}_2^+$  for which the vibrational hyperpolarizability is 10 times larger than the electronic one.<sup>21,22</sup> Some other examples, where the vibrational hyperpolarizability is significant but less spectacular, have already been reported (e.g.,  $\text{NH}_3^{23}$ ,  $\text{CH}_4^{23}$ ,  $\text{Li}_2^{24}$ , and  $\text{LiH}^{25}$ ). Bishop and Dalskov<sup>23a</sup> recently presented a survey of methods by which one can calculate the vibrational contributions to polarizabilities and hyperpolarizabilities.

Bishop and Kirtman,<sup>12a-c</sup> whose approach we employ in this work, define the vibrational contributions to the polarizability and second hyperpolarizability,  $\alpha^v$  and  $\gamma^v$ , respectively, by

$$\begin{aligned} \alpha^v &= [\mu_2]^{0,0} + [\mu^2]^{2,0} + [\mu^2]^{1,1}, \\ \gamma^v &= [\alpha^2]^{0,0} + [\alpha^2]^{2,0} + [\alpha]^{1,1} + [\mu\beta]^{0,0} \\ &\quad + [\mu\beta]^{2,0} + [\mu\beta]^{1,1} + [\mu^2\alpha]^{1,0} \\ &\quad + [\mu^2\alpha]^{0,1} + [\mu^4]^{2,0} + [\mu^4]^{1,1}. \end{aligned}$$

Expressions for  $[A]^{i,j}$ , where  $i$  and  $j$  denote orders of electrical and mechanical anharmonicity, respectively, were given by Bishop and Kirtman.<sup>12c</sup> These authors considered  $i \leq 2$  and  $j \leq 1$ . In the present work we took into account quadratic and cubic energy derivatives ( $m = 0, 1$ ), first- and second-order dipole moment derivatives ( $n = 1, 2$ ), first- and second-order polarizability derivatives ( $o = 1, 2$ ), and first-order hyperpolarizability derivatives ( $p = 1$ ). The various levels of anharmonicity considered in this work are denoted by ( $mnp$ ).

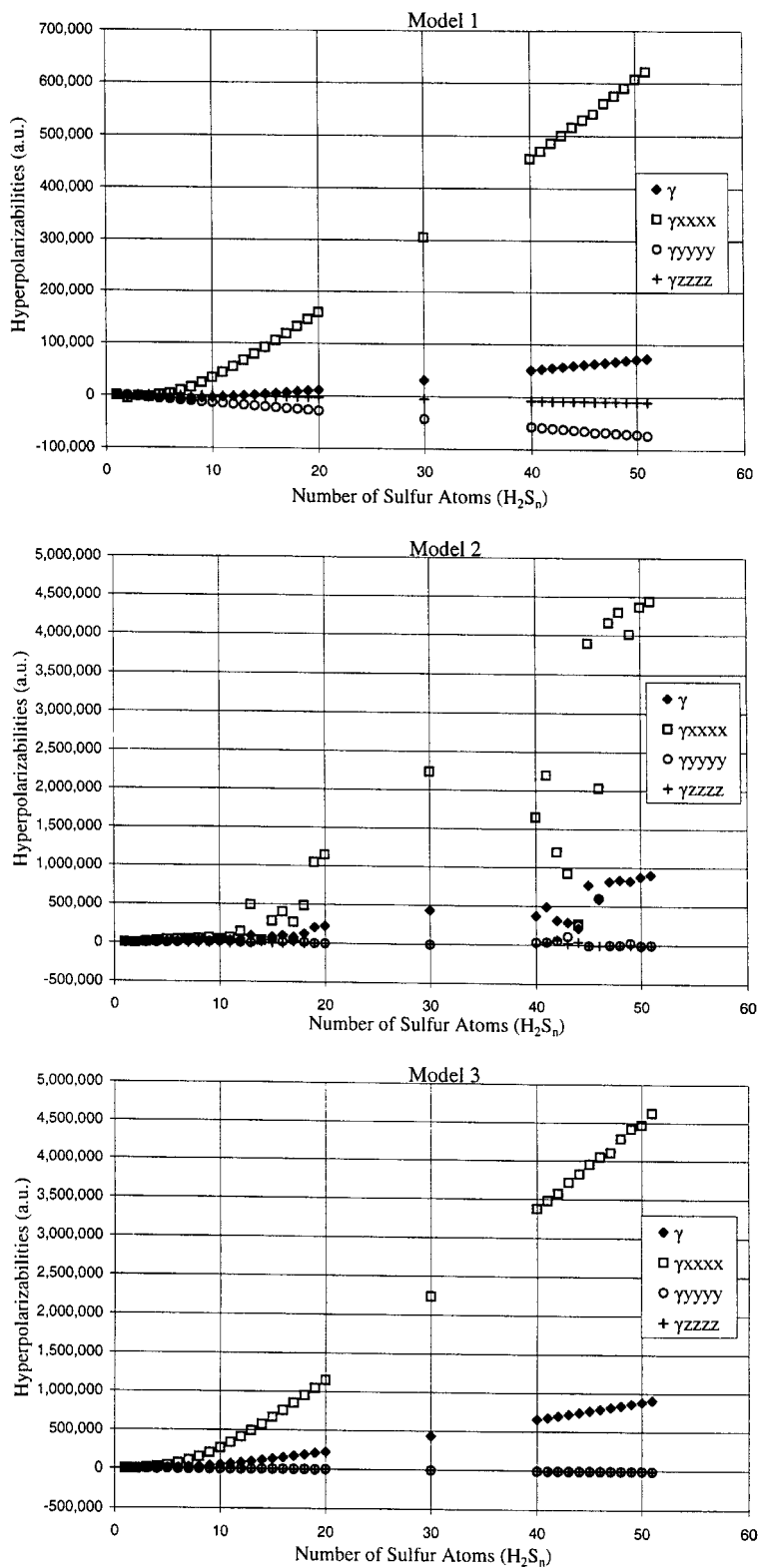


**FIGURE 8.** The hyperpolarizabilities ( $\gamma_{xxxx}$ ,  $\gamma_{yyyy}$ ,  $\gamma_{zzzz}$  and  $\gamma$ ) of models 1–3. The properties were calculated using the MNDO technique.

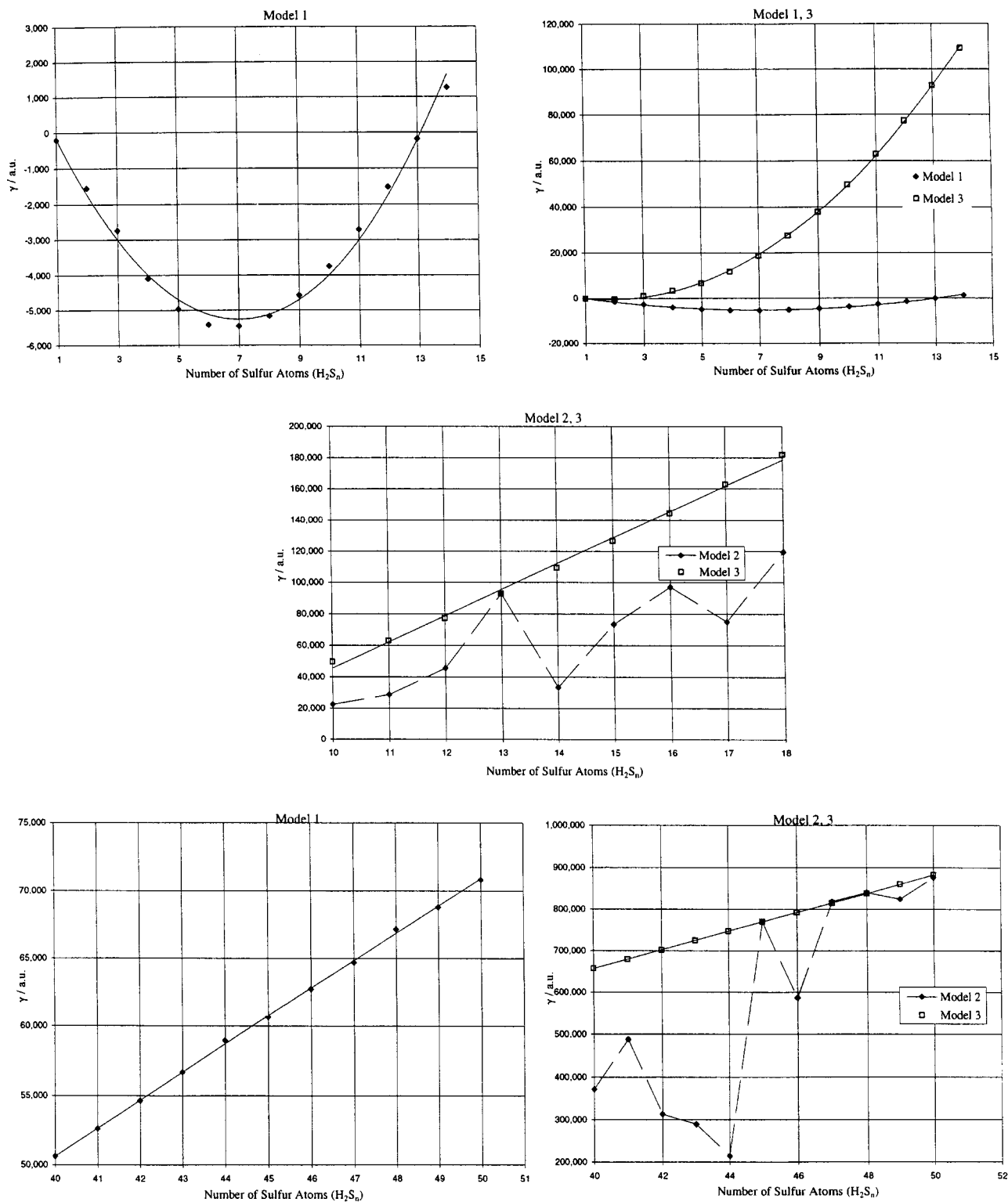


**FIGURE 9.** A comparative study of  $\gamma$  (MNDO) of  $\text{H}_2\text{S}_n$  for models 1–3.

TABLE IV. Comparison of Polarizabilities of Models 1 – 4.

No. Sulfur Atoms	$\alpha$ / au			
	$H_2S_n$			$S_n$
	Model 1	Model 2	Model 3	Model 4
8	119	115	126	108
12	190	189	206	174
16	262	267	287	241
20	335	370	370	308

These computations were performed by using the MNDO<sup>6</sup> method.

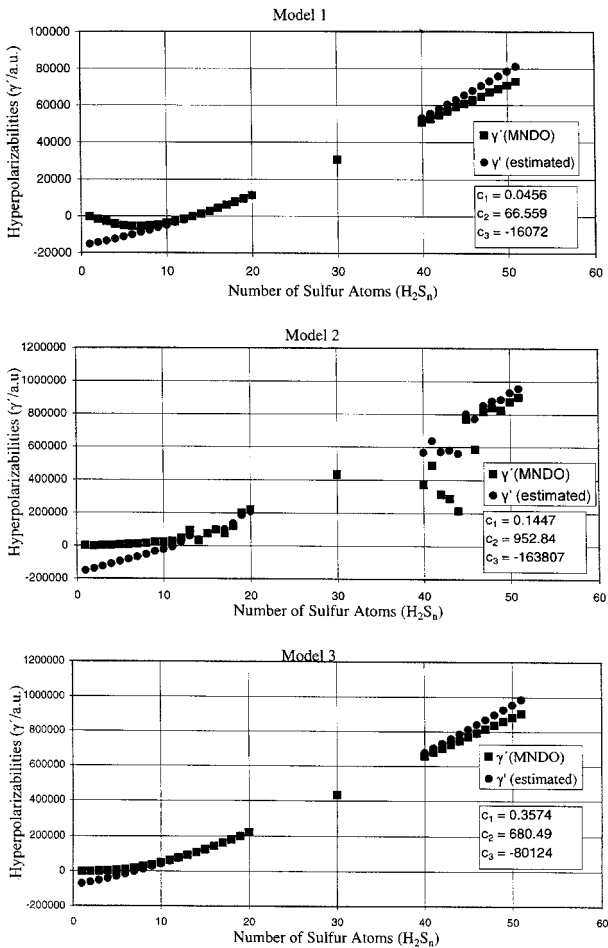


FIGURE 10.  $\gamma'$ (=  $\gamma$ /au) values of  $H_2S_n$ ,  $n = 1-12$  and 40–51, estimated by using the formula  $\gamma' = c_1\alpha'^2 + c_2\alpha' + c_3$  where  $\alpha' = \alpha$  / au The constants are determined from least squares fitting using the  $\alpha'$  and  $\gamma'$  values of  $H_2S_n$ ,  $n = 13-20$  and 30.

TABLE V. Comparison of Second Hyperpolarizabilities of Models 1 – 4.

No. Sulfur Atoms	$\gamma \times 10^{-2}$ / au			
	$H_2S_n$			$S_n$
	Model 1	Model 2	Model 3	Model 4
8	−51.7	139	275	13.1
12	−15.2	455	773	191
16	44.3	970	1440	400
20	114	2210	2210	676

The MNDO<sup>6</sup> method was used for these computations.

The static and dynamic (at 694.3 nm)  $\alpha^v$  and  $\gamma^v$  of  $H_2S$ ,  $H_2S_2$ , and  $H_2S_3$  are reported in Tables V and VI. Specifically, the contribution related to the electric field induced second harmonic generation (ESHG),  $\gamma^v(-2\omega;0,\omega,\omega)$ , is presented. These computations were performed at the SCF level using the contracted Gaussian type orbitals  $[3s2p/7s5p2d]$  suggested by Sadlej.<sup>10</sup>

We observe from Table VI that  $\alpha^v(0;0)$  increases with  $n$  ( $H_2S_n$ ). Indeed the static vibrational polarizability is zero for  $H_2S$  and almost negligible for  $H_2S_2$  but becomes a more substantial contribution for  $H_2S_3$ . For all three molecules, the dynamic property  $\alpha^v(-\omega;\omega)$  is zero at the selected frequency.

As expected, the results for  $\gamma^v$  of  $H_2S^n$  ( $n = 1-3$ ) are more interesting. We observe from Table VII that  $\gamma^v(0;0,0,0)$  is small but not negligible for  $H_2S$  and increases dramatically with  $n$ ; it is almost half the  $\gamma^e$  for  $H_2S_2$ , while for  $H_2S_3$  it exceeds the electronic contribution. We found that  $\gamma^v(-2\omega;0,\omega,\omega)$  is very small for  $H_2S_n$  ( $n = 1-3$ ). A similar observation was made by Bishop and Dalskov<sup>23a</sup> for  $CH_4$ ,  $NH_3$ ,  $H_2O$ , and  $HF$ , who

TABLE VI. Static and Frequency Dependent<sup>a</sup> Electronic and Vibrational Contribution to Polarizabilities of  $H_2S$ ,  $H_2S_2$ , and  $H_2S_3$ <sup>b</sup> Computed at SCF Level.

	$\alpha^e(0;0)$ /au	$\alpha^v(0;0)$ /au	$\alpha^3(-\omega;\omega)$ /au	$\alpha^v(-\omega;\omega)$ /au
$H_2S$	23.2	0.0	23.7	0.0
$H_2S_2$	40.5	0.9	41.4	0.0
$H_2S_3$	59.8	4.3	61.2	0.0

<sup>a</sup> At 694.3 nm.  
<sup>b</sup> Basis set:  $[3s2p/7s5p2d]$ .<sup>10</sup>

**TABLE VII.** Static and Frequency Dependent<sup>a</sup> Electronic and Vibrational Contribution to Second Hyperpolarizabilities of H<sub>2</sub>S, H<sub>2</sub>S<sub>2</sub>, and H<sub>2</sub>S<sub>3</sub><sup>b</sup>, Computed at SCF Level.

	$\gamma(0; 0, 0, 0)$ $\times 10^{-2} / \text{au}$	$\gamma^v(0; 0, 0, 0)$ $\times 10^{-2} / \text{au}$	$\gamma^e(-2\omega; 0, \omega, \omega)$ $\times 10^{-2} / \text{au}$	$\gamma^v(-2\omega; 0, \omega, \omega)$ $\times 10^{-2} / \text{au}$
H <sub>2</sub> S	53.8	6.8	78.2	-0.2
H <sub>2</sub> S <sub>2</sub>	83.2	38.2	119	-0.1
H <sub>2</sub> S <sub>3</sub>	136	171	199	2.8

<sup>a</sup> At 694.3 nm.

<sup>b</sup> Basis set: [3s2p/7s5p2d].<sup>10</sup>

found that  $\gamma^v(-2\omega; 0, \omega, \omega)$  for the above molecules was less than 5% of the corresponding  $\gamma^e$ . It is useful to note that the ratio of static contributions to the hyperpolarizability  $\gamma^e/\gamma^v$  are 9.4 and 7.9, for H<sub>2</sub>O<sup>23</sup> and H<sub>2</sub>S, respectively. Tentative computations of the static  $\gamma^v$  of H<sub>2</sub>S<sub>4</sub> confirm the above findings and show that it is 256% of  $\gamma^e$ .

To gain some insight into  $\alpha^v$  (static) and in particular  $\gamma^v$  (static), it is useful to analyze these properties at various anharmonicity levels. From the results of Table VIII we observe that  $\alpha^v$  shows small variation with (mnop). Harmonic potential approximation appears to adequately describe  $\alpha^v$  for H<sub>2</sub>S and H<sub>2</sub>S<sub>2</sub>. For H<sub>2</sub>S<sub>3</sub>, adding cubic terms leads to a small increase in  $\alpha^v$ . For both  $m = 0$  and  $m = 1$ , electrical anharmonicity has no effect on  $\alpha^v$ . In contrast,  $\gamma^v$  shows considerable dependence on the level of electrical anharmonicity, particularly for H<sub>2</sub>S<sub>3</sub>. However, although derivatives of  $\alpha$  appear to have a significant effect on  $\gamma^v$ , the first-order derivatives of  $\beta$  appear to be less important; for example, the difference between levels (1210)

and (1220) far exceeds that between (1220) and (1221). This observation is interesting because the first hyperpolarizability of H<sub>2</sub>S is not satisfactorily described at the Hartree–Fock level using the employed basis set. However, the reduced effect of first-order derivatives of  $\beta$  may be associated with the fact that out of the 10 terms  $[A]^{i,j}$  that describe  $\gamma^v$  in eq. (3), only two terms involve the first hyperpolarizability derivatives (first order)  $[\mu\beta]^{0,0}$  and  $[\mu\beta]^{1,1}$ . The term  $[\mu\beta]^{2,0}$  involves second-order derivatives of the first hyperpolarizability, which are not considered in this work.

Summarizing the results of this section, we note that  $\gamma^v$  (static) of H<sub>2</sub>S<sub>n</sub> makes a significant contribution to the second hyperpolarizability, except for H<sub>2</sub>S, where it is small but not negligible.

## Synopsis and Conclusions

We used several theoretical *ab initio* and semiempirical methods to systematically study the way in which the variation of the geometry of

**TABLE VIII.** Static  $\alpha^v$  and  $\gamma^v$  of H<sub>2</sub>S<sub>n</sub> ( $n = 1 - 3$ ) Calculated at Various Levels of Anharmonicity.

(mnop) <sup>a</sup>	H <sub>2</sub> S		H <sub>2</sub> S <sub>2</sub>		H <sub>2</sub> S <sub>3</sub>	
	$\alpha / \text{au}$	$\gamma \times 10^{-2} / \text{au}$	$\alpha / \text{au}$	$\gamma \times 10^{-2} / \text{au}$	$\alpha / \text{au}$	$\gamma \times 10^{-2} / \text{au}$
(0200)	0.01	0.00	0.85	1.68	4.11	25.1
(0210)	0.01	6.58	0.85	27.7	4.11	68.6
(0220)	0.01	6.68	0.85	42.4	4.11	163
(0221)	0.01	6.62	0.85	43.0	4.11	176
(1200)	0.01	0.00	0.86	2.67	4.26	59.2
(1210)	0.01	6.58	0.86	23.3	4.26	69.5
(1220)	0.01	6.83	0.86	37.7	4.26	159
(1221)	0.01	6.77	0.86	38.2	4.26	171

<sup>a</sup> (mnop) defines the order of anharmonicity. Specifically,  $m$ ,  $n$ ,  $o$ , and  $p$  defines the order of energy, the dipole moment, the polarizability, and the hyperpolarizability derivatives, respectively. The maximum anharmonicity employed in this work is (1221).



$H_2S_n$  affects their properties ( $\alpha_{ii}$ ,  $\alpha$ ,  $\gamma_{iiii}$ , etc.) and to comment on the implications of our observations. The *ab initio* study involved the computation of the static and frequency dependent electronic and vibrational contributions to the polarizabilities and second hyperpolarizabilities of several members of the series  $H_2S_n$ . Two basis sets were employed (STO-3G\*\*++ and [3s2p/7s5p2d]). Correlation was taken into account for some of the derivatives by using the MP2 theory. At the semiempirical level the MNDO<sup>6</sup> and MNDO/*d*<sup>7</sup> methods were used. Of primary importance for the present work are trends and differences, the validity of which is safeguarded to a great extent by the considered variety of methods. The main findings of the present work follow.

There is a similarity in the variation of the pairs  $\alpha_{ii}/\gamma_{iiii}$  and  $\alpha/\gamma$  of  $H_2S_n$  with  $n$ , which may be explained by taking into account that there is no charge transfer in the considered molecules. This observation may be used to predict the second hyperpolarizabilities if the polarizabilities (which require much lower computational cost) are known. We demonstrated that the longitudinal component has the dominant contribution to the polarizability and second hyperpolarizability of  $H_2S_n$ . A similar conclusion was reached for the contribution of this component to the average second hyperpolarizability of polyenic chains.<sup>13e</sup>

In the considered set of test molecules ( $H_2S_n$ ) a remarkable variation of the hyperpolarizabilities with the geometries was found. This result is significant because it shows that molecular geometry is an important tool for designing nonlinear optical materials.

The vibrational hyperpolarizabilities  $\gamma^v$  (static) of  $H_2S_n$  increase with  $n$ , and for  $H_2S_3$  it was demonstrated that  $\gamma^v > \gamma^e$ . The present results, in connection with those found in the literature, suggest that  $\gamma^v$  (static) should be computed whenever one aims at reasonably accurate molecular hyperpolarizabilities. Our values for  $\gamma^v(-2\omega; 0, \omega, \omega)$  are only a small percentage of  $\gamma^e$ . Studies on other molecules also found that the  $\gamma^v$  associated with ESHG is small.

## Acknowledgments

M. G. P. thanks Professor W. Thiel for providing him with a copy of his MNDO/*d* program, Professor N. C. Handy and Drs. A. Willetts and R. D. Amos for allowing him to use their programs

(CADPAC and SPECTRO), and Professor D. M. Bishop for sending him a preprint of his review article in *Advances in Chemical Physics*. We also thank Dr. V. E. Ingamells for reading the manuscript and making useful suggestions.

## References

- (a) The mean polarizability  $\alpha$  is defined by  $\alpha = \frac{1}{3}(\alpha_{xx} + \alpha_{yy} + \alpha_{zz})$ , where the suffixes  $x$ ,  $y$ , and  $z$  denote Cartesian components. The average second hyperpolarizability is determined by:  $\gamma = \frac{1}{15}(\gamma_{xxxx} + \gamma_{yyyy} + \gamma_{zzzz} + 2\gamma_{xxyy} + 2\gamma_{xxzz} + 2\gamma_{yyzz})$ ; (b) M. P. Bogaard and B. J. Orr, In *Physical Chemistry, Series Two*, vol. 2, A. D. Buckingham, Ed., MTP International Review of Science, Butterworths, London, 1975, p. 149; (c) A. D. Buckingham and B. J. Orr, *Quantum Rev. Chem. Soc.*, **21**, 195 (1967).
- (a) S. M. Le Cours, H.-W. Guan, S. G. Di Magno, C. H. Wang, and M. J. Thierien, *J. Am. Chem. Soc.*, **118**, 1497 (1996); (b) S. Priyadarshy, M. J. Thierien, and D. N. Beratan, *J. Am. Chem. Soc.*, **118**, 1504 (1996); (c) P. Norman, D. Jonsson, O. Vahtras, and H. Ågren, *Chem. Phys.*, **203**, 23 (1996).
- (a) M. Nakano, S. Yamada, I. Shigemoto, and K. Yamaguchi, *Chem. Phys. Lett.*, **250**, 247 (1996); (b) Z. Shuai, S. Ramasesha, and J. L. Brédas, *Chem. Phys. Lett.*, **250**, 14 (1996); (c) F. Aiga and R. Itoh, *Chem. Phys. Lett.*, **251**, 372 (1996); (d) M. Nakano, S. Yamada, I. Shigemoto, and K. Yamaguchi, *Chem. Phys. Lett.*, **251**, 381 (1996); (e) M. L. Dekhtyar and V. M. Rozenbaum, *J. Phys. Chem.*, **101**, 809 (1997); (f) P. Norman, Y. Luo, D. Jonsson, and H. Ågren, *J. Chem. Phys.*, **106**, 1827 (1997); (g) J. O. Morley, *Int. J. Quantum Chem.*, **61**, 991 (1997); (h) B. Kirtman, B. Champagne, and J.-M. André, *J. Chem. Phys.*, **104**, 4125 (1996); (i) D. P. Shelton and J. E. Rice, *Chem. Rev.*, **94**, 3 (1994); (j) D. R. Kanis, P. G. Lacroix, M. A. Ratner, and T. J. Marks, *J. Am. Chem. Soc.*, **116**, 10089 (1994); (k) D. Mukhopadhyay and Z. G. Soos, *J. Chem. Phys.*, **104**, 1600 (1996); (l) S. R. Marder, W. E. Torruellas, M. Blanchard-Desce, V. Ricci, G. I. Stegeman, S. Gilmour, J.-L. Brédas, J. Li, G. U. Bublitz, and S. G. Boxer, *Science*, **276**, 1233 (1997); (m) J. L. Toto, T. T. Toto, C. P. de Melo, B. Kirtman, and K. Robins, *J. Chem. Phys.*, **104**, 8586 (1996).
- (a) D. J. Williams, Ed., *Nonlinear Optical Properties of Organic and Polymeric Materials*, American Chemical Society, Washington, D.C., 1983; (b) S. R. Marder and J. W. Perry, *Science*, **263**, 1706 (1994); (c) P. N. Prasad and D. J. Williams, *Introduction to Nonlinear Optical Effects in Molecules and Polymers*, Wiley, New York, 1991.
- (a) C. J. Marsden and B. S. Smith, *J. Phys. Chem.*, **92**, 347 (1988); (b) A. Rauk, *J. Am. Chem. Soc.*, **106**, 6517 (1984); (c) D. Beljonne, Z. Shuai, and J. L. Brédas, *J. Chem. Phys.*, **98**, 8819 (1993); (d) M. G. Papadopoulos and J. Waite, *Nonlinear Opt.*, **7**, 65 (1994); (e) S. R. Marder, J. W. Perry, G. Bourhill, C. B. Gorman, B. G. Tiemann, and K. Mansour, *Science*, **261**, 186 (1993); (f) B. Kirtman, *Chem. Phys. Lett.*, **143**, 81 (1988); (g) G. J. B. Hurst, M. Dupuis, and E. Clementi, *J. Chem. Phys.*, **89**, 385 (1988); (h) C. P. De Melo and R. Silbey, *Chem. Phys. Lett.*, **140**, 537 (1987); (i) B. Kirtman and M. Hasan,

- Chem. Phys. Lett.*, **157**, 123 (1989); (j) D. Li, M. A. Ratner, and T. J. Marks, *J. Am. Chem. Soc.*, **110**, 1707 (1988); (k) Y.-J. Lu and S. L. Lee, *Int. J. Quantum Chem.*, **44**, 773 (1992); (l) Z. Huang, D. A. Jelski, R. Wang, D. Xie, C. Zhao, X. Xia, and T. F. George, *Can. J. Chem.*, **70**, 372 (1992).
6. (a) M. J. S. Dewar and W. Thiel, *J. Am. Chem. Soc.*, **99**, 4899 (1977); (b) J. J. P. Stewart and F. J. Seiler, *MOPAC 6.00*, Research Laboratory, United States Air Force Academy, 1990.
  7. (a) W. Thiel and A. A. Voityuk, *Theor. Chim. Acta*, **81**, 391 (1992); (b) W. Thiel and A. A. Voityuk, *J. Phys. Chem.*, **100**, 616 (1996); (c) M. Malagoli and W. Thiel, *Chem. Phys.*, **206**, 73 (1996).
  8. C. Møller and M. S. Plesset, *Phys. Rev.*, **46**, 618 (1934).
  9. M. W. Schmidt, K. K. Baldrige, J. A. Boatz, S. T. Elbert, M. S. Gordon, J. H. Jensen, S. Kozeki, N. Matsunaga, K. A. Nguyen, S. J. Su, T. L. Windus, M. Dupuis, and J. A. Montgomery, *J. Comput. Chem.*, **14**, 1347 (1993).
  10. (a) A. J. Sadlej, *Col. Cz. Chem. Com.*, **53**, 1995 (1988); (b) A. J. Sadlej, *Theor. Chim. Acta*, **79**, 123 (1991).
  11. H. A. Kurtz, J. J. P. Stewart, and K. M. Dieter, *J. Comput. Chem.*, **11**, 82 (1990).
  12. (a) B. Kirtman and D. M. Bishop, *Chem. Phys. Lett.*, **175**, 601 (1990); (b) D. M. Bishop and B. Kirtman, *J. Chem. Phys.*, **95**, 2646 (1991); (c) D. M. Bishop and B. Kirtman, *J. Chem. Phys.*, **97**, 5255 (1992); (d) M. J. Cohen, A. Willetts, R. D. Amos, and N. C. Handy, *J. Chem. Phys.*, **100**, 4467 (1994); (e) R. D. Amos, I. L. Alberts, J. S. Andrews, S. M. Colwell, N. C. Handy, D. Jayatilaka, P. J. Knowles, R. Kobayashi, N. Koga, K. E. Laidig, P. E. Maslen, C. W. Murray, J. E. Rice, J. Sanz, E. D. Simandiras, A. J. Stone, and M.-D. Su, *CADPAC, The Cambridge Analytic Derivatives Package Issue 5*, Cambridge, U.K., 1992; (f) A. Willetts, J. F. Gaw, W. H. Green, and N. C. Handy, In *Advances in Molecular Vibrations and Collision Dynamics*, vol. 1B, J. M. Bowman and M. A. Ratner, Eds., JAI Press, Greenwich, CT, 1991; (g) Conversion factors:
 

1 au dipole moment	~ 2.54174 D
	~ $8.47831 \times 10^{-30}$ C m
1 au of polarizability	~ $0.148176 \times 10^{-24}$ esu
	~ $0.164867 \times 10^{-40}$ C <sup>2</sup> m <sup>2</sup> J <sup>-1</sup>
1 au of second hyperpolarizability	~ $0.503717 \times 10^{-39}$ esu
	~ $0.623597 \times 10^{-64}$ C <sup>4</sup> m <sup>4</sup> J <sup>-3</sup>
  13. (a) A. Dulcic, C. Flytzanis, C. L. Tang, D. Pépin, M. Fetizon, and Y. Hoppilliard, *J. Chem. Phys.*, **74**, 1559 (1981); (b) C. Flytzanis, In *Nonlinear Behaviour of Molecules, Atoms and Ions in Electric, Magnetic or Electromagnetic Fields*, L. Neel, Ed., Elsevier, Amsterdam, 1979; (c) J. P. Hermann and J. Ducuing, *J. Appl. Phys.*, **45**, 5100 (1974); (d) V. Dobrosavljević and R. M. Strat, *Phys. Rev. B*, **35**, 2781 (1987); (e) C. P. de Melo and R. Silbey, *J. Chem. Phys.*, **88**, 2567 (1988); (f) S. R. Marder, L.-T. Cheng, B. G. Tiemann, A. C. Friedli, M. Blanchard-Desce, J. W. Perry, and J. Skindhøj, *Science*, **263**, 511 (1994); (g) C. B. Gorman and S. R. Marder, *Proc. Natl. Acad. Sci.*, **90**, 11297 (1993); (h) D. R. Kanis, M. A. Ratner, and T. J. Marks, *Chem. Rev.*, **94**, 195 (1994); (i) I. D. W. Samuel, I. Ledoux, C. Dhenaut, J. Zyss, H. H. Fox, R. R. Schrock, and R. J. Silbey, *Science*, **265**, 1070 (1994).
  14. S. Tretiak, V. Chernyak, and S. Mukamel, *Phys. Rev. Lett.*, **77**, 4656 (1996).
  15. (a) S. N. Yaliraki and R. J. Silbey, *J. Chem. Phys.*, **104**, 1245 (1996); (b) D. M. Bishop, *Adv. Chem. Phys.*, to appear; (c) B. Kirtman and B. Champagne, *Int. Rev. Phys. Chem.*, **16**, 389 (1997).
  16. (a) S. M. Nasiou, I. N. Demetropoulos, M. G. Papadopoulos, and S. Raptis, *16th Panhellenic Conference of Chemistry*, 1995, p. 858; (b) Serena Software, Bloomington, IN; (c) N. L. Allinger, *J. Am. Chem. Soc.*, **99**, 8127 (1977); (d) U. Burkert and N. L. Allinger, *Molecular Mechanics*, ACS Monograph 177, American Chemical Society, Washington, D.C., 1982; (e) M. Saunders, K. N. Houk, Y. D. Wu, W. C. Still, M. Lipton, G. Chang, and W. C. Guida, *J. Am. Chem. Soc.*, **112**, 1419 (1990).
  17. N. N. Greenwood and A. Earnshaw, *Chemistry of the Elements*, Pergamon, Oxford, U.K., 1985.
  18. (a) F. A. Cotton and G. Wilkinson, *Advanced Inorganic Chemistry*, 5th ed., Wiley, New York, 1988, p. 495: "When molten sulfur is poured into ice water, the so-called plastic sulfur is obtained; although normally this has S<sub>8</sub> inclusions, it can be obtained as long fibers by heating S<sub>8</sub> in nitrogen at 300°C for 5 min and quenching a thin stream in ice water. These fibers can be stretched under water and appear to contain helical chains of sulfur atoms with ~ 3.5 atoms per turn." (b) I. Mayer, *J. Mol. Struct. (Theochem.)*, **149**, 81 (1987); (c) B. Meyer, *Chem. Rev.*, **76**, 367 (1976); (d) K. Steliou, *Acc. Chem. Res.*, **24**, 341 (1991); (e) G. P. Agrawal, C. Cojan, and C. Flytzanis, *Phys. Rev. B*, **17**, 776 (1978).
  19. (a) J. W. Ward and C. K. Miller, *Phys. Rev. A*, **19**, 826 (1979); (b) A. L. McClellan, *Tables of Experimental Dipole Moments*, W. H. Freeman, London, 1963; (c) N. Matzuzawa and D. A. Dixon, *Int. J. Quantum Chem.*, **44**, 497 (1992); (d) H. Sekino and R. J. Bartlett, *J. Chem. Phys.*, **98**, 3022 (1993).
  20. D. M. Bishop, *Rev. Modern Phys.*, **62**, 343 (1990).
  21. D. P. Shelton and L. Ulivi, *J. Chem. Phys.*, **89**, 149 (1988).
  22. D. M. Bishop, J. Pipin, and J. N. Silverman, *Mol. Phys.*, **59**, 165 (1986).
  23. (a) D. M. Bishop and E. K. Dalskov, *J. Chem. Phys.*, **104**, 1004 (1996); (b) D. M. Bishop, B. Kirtman, H. A. Kurtz, and J. E. Rice, *J. Chem. Phys.*, **98**, 8024 (1993).
  24. M. G. Papadopoulos, A. Willetts, N. C. Handy, and A. D. Buckingham, *Mol. Phys.*, **85**, 1193 (1995).
  25. M. G. Papadopoulos, A. Willetts, N. C. Handy, and A. E. Underhill, *Mol. Phys.*, **88**, 1063 (1996).
  26. M. P. Bogaard, A. D. Buckingham, R. K. Pierens, A. W. White, *Trans. Faraday Soc. I*, **74**, 3008 (1978).